Ecotoxicology and Environmental Safety 242 (2022) 113939

Contents lists available at ScienceDirect

Ecotoxicology and Environmental Safety

journal homepage: www.elsevier.com/locate/ecoenv

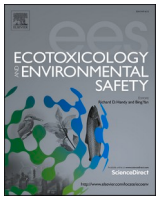

In vivo phytotoxic effect of yttrium-oxide nanoparticles on the growth, uptake and translocation of tomato seedlings (*Lycopersicon esculentum*)

Xueping Wang [a,b], Xiaojie Liu [a], Xiao Yang [a,b], Lingqing Wang [a,b,*], Jun Yang [a], Xiulan Yan [a], Tao Liang [a,b], Hans Chr. Bruun Hansen [b,c], Balal Yousaf [d], Sabry M. Shaheen [e,f,g,1], Nanthi Bolan [h], Jörg Rinklebe [e,i,2]

[a] *Key Laboratory of Land Surface Pattern and Simulation, Institute of Geographic Sciences and Natural Resources Research, Chinese Academy of Sciences, Beijing 100101, China*

[b] *Sino-Danish College, University of Chinese Academy of Sciences, Beijing 100049, China*

[c] *Department of Plant and Environmental Sciences, University of Copenhagen, Thorvaldsensvej 40, DK-1871 Frederiksberg C, Denmark*

[d] *CAS-Key Laboratory of Crust-Mantle Materials and the Environments, School of Earth and Space Sciences, University of Science and Technology of China, Hefai 230026, Anhui, China*

[e] *University of Wuppertal, School of Architecture and Civil Engineering, Institute of Foundation Engineering, Water, and Waste-Management, Laboratory of Soil, and Groundwater-Management, Pauluskirchstraße 7, 42285 Wuppertal, Germany*

[f] *King Abdulaziz University, Faculty of Meteorology, Environment, and Arid Land Agriculture, Department of Arid Land Agriculture, Jeddah 21589, Saudi Arabia*

[g] *University of Kafrelsheikh, Faculty of Agriculture, Department of Soil and Water Sciences, 33 516 Kafr El-Sheikh, Egypt*

[h] *UWA School of Agriculture and Environment, UWA Institute of Agriculture, The University of Western Australia, Perth, WA 6001, Australia*

[i] *International Research Centre of Nanotechnology for Himalayan Sustainability (IRCNHS), Shoolini University, Solan 173212, Himachal Pradesh, India*

A R T I C L E I N F O

Edited by Dr. Muhammad Zia-ur-Rehman

Keywords:
Yttrium oxide nanoparticles
Phytotoxicology
Translocation
Tomato (*Lycopersicon esculentum*)
Rare earth elements

A B S T R A C T

The potential toxicity and ecological risks of rare-earth nanoparticles in the environment have become a concern due to their widespread application and inevitable releases. The integration of hydroponics experiments, partial least squares structural equation modeling (PLS-SEM), and Transmission Electron Microscopy (TEM) were utilized to investigate the physiological toxicity, uptake and translocation of yttrium oxide nanoparticles (Y_2O_3 NPs) under different hydroponic treatments (1, 5, 10, 20, 50 and 100 mg·L^{-1} of Y_2O_3 NPs, 19.2 mg·L^{-1} $Y(NO_3)_3$ and control) in tomato (*Lycopersicon esculentum*) seedlings. The results indicated that Y_2O_3 NPs had a phytotoxic effect on tomato seedlings' germination, morphology, physiology, and oxidative stress. The Y_2O_3 NPs and soluble Y^{III} reduced the root elongation, bud elongation, root activity, chlorophyll, soluble protein content and superoxide dismutase and accelerated the proline and malondialdehyde in the plant with increasing concentrations. The phytotoxic effects of Y_2O_3 NPs on tomato seedlings had a higher phytotoxic effect than soluble Y^{III} under the all treatments. The inhibition rates of different levels of Y_2O_3 NPs in shoot and root biomass ranged from 0.2% to 6.3% and 1.0–11.3%, respectively. The bioaccumulation and translocation factors were less than 1, which suggested that Y_2O_3 NPs significantly suppressed shoot and root biomass of tomato seedlings and easily bioaccumulated in the root. The observations were consistent with the process of concentration-dependent uptake and translocation factor and confirmed by TEM. Y_2O_3 NPs penetrate the epidermis, enter the cell wall, and exist in the intercellular space and cytoplasm of mesophyll cells of tomato seedlings by endocytic pathway. Moreover, PLS-SEM revealed that the concentration of NPs significantly negatively affects the morphology and physiology, leading to the change in biomass of plants. This study demonstrated the possible pathway of Y_2O_3 NPs in uptake, phytotoxicity and translocation of Y_2O_3 NPs in tomato seedlings.

* Corresponding author at: Key Laboratory of Land Surface Pattern and Simulation, Institute of Geographic Sciences and Natural Resources Research, Chinese Academy of Sciences, Beijing 100101, China.

E-mail addresses: wanglq@igsnrr.ac.cn (L. Wang), shaheen@uni-wuppertal.de (S.M. Shaheen), rinklebe@uni-wuppertal.de (J. Rinklebe).

[1] ORCID: 0000-0002-5618-8175

[2] ORCID: 0000-0001-7404-1639

https://doi.org/10.1016/j.ecoenv.2022.113939

Received 7 May 2022; Received in revised form 20 July 2022; Accepted 29 July 2022

Available online 2 August 2022

1. Introduction

Nanoparticles (NPs) have drawn public attention because of their unique physicochemical properties and extensive applications in a variety of fields (Rajput et al., 2018). With the rapid growth of NPs production and applications worldwide, NPs have played a primary part in society and remarkably affect technical advances (Peijnenburg et al., 2016). The most frequent application of NPs in daily life are generally titanium, lead, copper and some rare earth elements (-oxides) (Courtois et al., 2019; Hou et al., 2017; Ullah et al., 2020). Rare earth elements (REEs) have become an important part of modern technologies, finding various routes into different environmental media (Khanna et al., 2021; Tian et al., 2018). For example, high contents of REEs have been found in atmospheric particulates (63.23–105.52 $ng{\cdot}m^{-3}$), freshwater lake sediment (145.1–351.1 $\mu g{\cdot}g^{-1}$), ocean bottom sediment (ΣREEs < 2511 $mg{\cdot}kg^{-1}$) and soil (122–825 $\mu mol{\cdot}kg^{-1}$), contributing to environmental pollution, ecological risks and human health (Balaram, 2019; Mihajlovic et al., 2017; Wang et al., 2014, 2019).

Rare earth oxide nanoparticles (REONPs) are abundant in nature and manufactured at a large-scale such as for application in coatings, polishing powders, automotive exhaust catalysts, nanoparticles-containing biosolid, fertilizer and pesticides (Qi et al., 2019; Younis et al., 2021). Yttrium oxide nanoparticles (Y_2O_3 NPs) are among the most important yttrium compounds and are representative of heavy REONPs (Yu et al., 2020). Most Y_2O_3 NPs are used in manufacture of catalysts, in synthesis, and for biological applications (Chen et al., 2016; Gong et al., 2019). The wide application of Y_2O_3 NPs inevitably spread into the ecosystem as dust or migrates to plants, animals and even people through water and soil during their production and waste treatment, causing potential effects on the ecological function and human health (Gong et al., 2019). For example, Y_2O_3 NPs (10–500 $mg{\cdot}L^{-1}$) inhibited the maize seed vitality and seedlings growth (Gong et al., 2019), 24-h incubation experiment revealed that Y_2O_3 NPs (12.5–50 $mg{\cdot}L^{-1}$) promote the apoptosis and decrease the cell survival (Selvaraj et al., 2014). Thus, it is important to assess the environmental risks of Y_2O_3 NPs and understand their fate and effects on the environment.

REONPs in soil interact with plants, adhere to the surface of roots, accumulate in plants, and affect growth and biochemical functioning (Spielman-Sun et al., 2019). REONPs and physical and chemical processes in plants lead to phytotoxicity, including many physiological and biochemical mechanisms in root and other plant tissues (Malandrakis et al., 2021). Some studies have been conducted on the interaction between NPs and plants. These reports indicated that REONPs directly or indirectly affect germination rate (Gong et al., 2019), root and shoot lengths (Ma et al., 2010), shoot and root biomass (Dong et al., 2021), as well as root morphology (López-Moreno et al., 2016). At the same time, the positive or negative impact of NPs on plant germination, photosynthesis and growth depend on the concentrations and mobility of NPs. For instance, CeO_2 NPs accelerated the growth of rice at 100 $mg{\cdot}kg^{-1}$ application rate while inhibited plant growth at a higher application rate of 500 $mg{\cdot}kg^{-1}$ (Zhang et al., 2021). Y_2O_3 NPs could delay germination by reducing seed vitality at 10–500 $mg{\cdot}L^{-1}$ (Gong et al., 2019). CeO_2 NPs reduced the fresh weight of plant shoot by 34.5% at 75 CeO_2 $mg{\cdot}kg^{-1}$ (Dong et al., 2021). Approximately 45.5% of NPs were detected in plant root, and about 0.6% of NPs were measured in leaves (Ma et al., 2010). CeO_2 NPs significantly adversely affect the antioxidant systems and photosystem of *Arabidopsis thaliana* at higher solution concentrations (2000 or 3000 $mg{\cdot}L^{-1}$) (Yang et al., 2017a, 2017b). However, the quantitative impact of REONPs on the morphology and phytotoxicity of plants is unclear. Advanced testing methods and appropriate model could provide a new insight to understand the toxicity mechanisms of REONPs on plants. Synchrotron dual-energy X-ray micro-tomography (Chen et al., 2016), nuclear magnetic resonance (Gong et al., 2019), and transmission electron microscopy (TEM) (Yang et al., 2017a, 2017b) have been applied to clarify the mechanism of phytotoxicity, uptake, and translocation of REONPs in plants. TEM is the most popular technique to capture fine detail—even as small as a single column of atoms, which has the potential to image the location of REONPs on a cellular scale (Yang et al., 2017a, 2017b). The impact of REONPs on plants manifests in changes of physical, chemical and biological functioning. The relationship between the REONPs and these plant functions may be quantified by partial least squares structural equation modeling (PLS-SEM), which is beneficial to understand the relationship between REONPs and their effects on plants (Wang et al., 2021).

Tomato (*Lycopersicon esculentum*) is a major vegetable or fruit crop with high nutrition and strong economic values, which also is one of the most consumed vegetables in the world. Some prior studies have investigated the effect of light REONPs (CeO_2, Gd_2O_3 and La_2O_3) on the phytotoxicity of tomato root elongation but paid little attention to the adsorption of NPs by plants (Ma et al., 2010; Mihajlovic et al., 2017). The interaction of Y_2O_3 NPs with other crops (such as rice and maize) (Gong et al., 2019; Zhao et al., 2021), and the effect of soluble Y^{III} released from the Y_2O_3 NPs have had only little attention in these studies. Thus, this present study aims to: (i) evaluate the phytotoxic effect of Y_2O_3 NPs and its released soluble Y^{III} complexes on the morphology, physiology, and oxidative stress of tomato seedlings in the germination and growth process, (ii) clarify the translocation and bioaccumulation mechanism in tomato seedlings, and (iii) identify the relationship between Y_2O_3 NPs and changes in plant properties.

2. Materials and methods

2.1. Nanoparticles and chemicals

The Y_2O_3 NPs were provided by Nanjing Hongde Nanomaterials Co., Ltd (Nanjing, China), which provided the results showed the mean particle size and specific surface area of purchased Y_2O_3 NPs were 20–30 nm (purity > 99.99%) and 61 $m^2{\cdot}g^{-1}$, respectively. $Y(NO_3)_3.6\,H_2O$ (analytical grades) were purchased by Nanjing Hongde Nanomaterials Co., Ltd (Nanjing, China), with a density of 2.7 $g{\cdot}mL^{-1}$ at 25 °C and solubility in water (100 mL) of 123 g at 20 ℃.

2.2. Plant germination

Material preparation: REEs have a hormesis effect on plant growth and development (Agathokleous et al., 2018). Previous studies revealed that Y_2O_3 NPs could promote plant growth at a low concentration (0–10 $mg{\cdot}L^{-1}$) (Gong et al., 2019). However, Y_2O_3 NPs had an inhibition effect on germination indexes of the plants when Y_2O_3 NPs concentrations exceeded 50 $mg{\cdot}L^{-1}$ (Gong et al., 2019; Yu et al., 2020). The positive or negative effect on seed germination and plant growth depends on the concentration of NPs (Xie et al., 2022). Therefore, the Y_2O_3 NPs concentrations in all treatments were set at 1, 5, 10, 20, 50 and 100 $mg{\cdot}L^{-1}$. Different concentration levels of Y_2O_3 NPs (0, 1, 5, 10, 20, 50 and 100 $mg{\cdot}L^{-1}$) were made by dilution with water. After ageing of the Y_2O_3 NP suspension for 3 days, the concentrations of soluble Y^{III} were 3.9, 5.0 and 6.2 $mg{\cdot}L^{-1}$, when the concentration of Y_2O_3 NPs suspensions were 20, 50 and 100 $mg{\cdot}L^{-1}$, respectively. Hence, the 100 $mg{\cdot}L^{-1}$ Y_2O_3 suspension was used to clarify the difference in translocation of Y_2O_3 NPs and Y^{III} species in plants.

Tomato seeds (*Lycopersicon esculentum*, Meiqi 1) with a germination rate of 90% were purchased from Yangling Agricultural High-tech Development Joint Stock Co., Ltd (Yangling, China). Approximately 26.7 mg of $Y(NO_3)_3.6\,H_2O$ was dissolved in 1 L of deionized water. The concentration of $Y(NO_3)_3$ and soluble Y^{III} in the $Y(NO_3)_3$ solution were 19.2 $mg{\cdot}L^{-1}$ and 6.2 $mg{\cdot}L^{-1}$, respectively. An aqueous suspension of Y_2O_3 NPs with a concentration of 100 $mg{\cdot}L^{-1}$ was prepared ultrasonically mixed for 30 min (100 W, 40 kHz). Different concentration levels of Y_2O_3 NPs (0, 1, 5, 10, 20, 50 and 100 $mg{\cdot}L^{-1}$) were made by dilution with water. The solution pH was approximately 6.8 only with 1/2 Hoagland nutrient solution in the control group, and the optimal pH for tomato growth is between 6.0 and 6.8 (Ovelar et al., 2021). Hence, the

solution pH of all treatments was adjusted to 6.8 ± 0.1.

Germination experiment: The tomato seeds were sterilized with NaClO for 30 min and washed with 20 mmol·L^{-1} Na_2-EDTA and ultrapure water. After that, the tomato seeds were soaked in 0, 1, 5, 10, 20, 50 and 100 mg·L^{-1} Y_2O_3 NPs suspension and 19.2 mg·L^{-1} $Y(NO_3)_3$ for 4 h. Then, 20 seeds were planted in Petri dishes that were added 15 mL Y_2O_3 NPs at the respective concentrations. All treatments were kept under ambient conditions (approximately 80% relative humidity, darkness and 25 ℃) for 7 days. When the length of the embryo reached half of the seed diameter, the seed was considered fully germinated (Zhao et al., 2021). The germinating seed numbers, shoot lengths, and root lengths were recorded every day.

2.3. Hydroponic culture experiment

The tomato seeds were sterilized with NaClO for 30 min and washed with 20 mmol·L^{-1} Na_2-EDTA and ultrapure water. After sterilization and washing, tomato seeds were soaked in ultrapure water for 4 h. Twenty seeds were then planted in seedling trays with vermiculite substrate and grown in a climate incubator until in two true leaf stage at 80% humidity and 25 °C with light (225 μmol·m^{-2}·s^{-1} for a 14/10 h light/dark cycle). Afterward, the seedlings were planted into Y_2O_3 NPs suspensions and Y $(NO_3)_3$ solution (mixed with 1/2 Hoagland's solution) for 15 days. All treatments were three replicates in a climate incubator. The suspensions were stirred with a glass rod about 6 times a day to prevent the agglomeration of Y_2O_3 NPs.

The tomato seedlings were removed from the nutrient solution and washed with ultrapure water. The roots were soaked in Na_2-EDTA (20 mmol·L^{-1}) for 30 min. This step aims to remove the Y_2O_3 NPs adhering to the root surface. Subsequently, the seedling roots were washed with ultrapure water. All samples of tomato seedlings were separated into root and shoot, and then their masses were weighed. Samples were dried at 105 °C for 35 min and then at 70 °C for 10 h (Zhao et al., 2021). After this, the mass of the dried biomasses were recorded.

2.4. Analyses

Proline is a critical substance in preventing membrane distortion and functional failures under stress (Lei et al., 2016). Malondialdehyde (MDA) is a lipid peroxidation product resulting from the oxidative attack on cell membrane phospholipids and circulating lipids. The two indicators can reflect plant membrane integrity and the degree of oxidative stress under the treatment with NPs (Dragun et al., 2017). Superoxide dismutase (SOD) is a crucial component of the antioxidant enzyme system in biological systems (Du et al., 2019).

Chlorophyll contents were extracted by acetone water solutions (80% v/v) in the dark and measured with a spectrophotometer at wavelengths of 663 nm, 645 nm and 470 nm (Iftikhar et al., 2019; Lichtenthaler, 1987). Proline was determined by the sulfosalicylic acid method (Zhao et al., 2021). Malondialdehyde (MDA) and SOD (superoxide dismutase) were measured with a thiobarbituric acid method and the nitroblue tetrazolium method, respectively (Dong et al., 2021). Coomassie Brilliant Blue G-250 was used to assess the soluble protein content (Zhao et al., 2021). Triphenyl tetrazolium chloride was used to test the root activity of tomato seedlings (Zhao et al., 2021). The details of the analytical methods (i.e., SOD, MDA and root activity) have been presented in previous studies (Dong et al., 2021; Zhao et al., 2021).

The yttrium concentrations in the root and shoot of tomato seedlings were measured using ICP-MS (Agilent 7700, USA); the details of the digestion process are listed in Supporting Information. For the distribution of yttrium in tomato seedlings, the samples were imaged by Transmission Electron Microscope (TEM) coupled with Energy Dispersive Spectrometer (EDS) (Tecnai G2 F20, USA). After exposure to 15 days, the leaves of tomato seedlings were washed and dried, and the leave samples then cut into small pieces of about 1 mm^2. Then the samples were immersed in phosphate buffer (pH=7, 0.1 M) containing 2.5% glutaraldehyde for more than 3.5 h and 1% osmic acid for 2 h. After these steps, the leave samples were dehydrated with a series of gradient concentrations (50%, 70%, 80%, 90%, 95%) of ethanol for 20 min and finally treated with 100% ethanol 3 times (20 min·treatment^{-1}). The sample was transfered to acetone solution and embedded in epoxy resin (ETON 812), and then sliced to 60–80 nm by an ultramicrotome. After double staining with uranyl acetate and lead citrate for 15 min, they were fixed on nickel grids, and the samples then analyzed by TEM.

2.5. Data analyses

In this study, the content of Y_2O_3 NPs in roots and shoots is expressed based on fresh weight (FW). The Michaelis-Menten equation was applied to represent the process of the concentration-dependent NP uptake of tomatoes.

$$V = V_{max}C/(K_t + C) \quad (1)$$

Where V and V_{max} are the uptake rate and maximum uptake rate (mg·(kg·h)$^{-1}$), respectively. C is the concentration of Y_2O_3 NPs in solution (Y_2O_3 NPs, mg·L^{-1}), and K_t is the Michaelis constant representing the substrate concentration at half of the maximum absorption rate (Wang et al., 2020).

Partial least squares structural equation modeling (PLS-SEM) is a statistical method for multivariate data analysis by hypotheses testing, focusing on mining sample information, and has no requirement for normal data distribution (Hair et al., 2019). Besides, PLS-SEM emphasizes prediction on estimating statistical models, which can construct both reflective or formative indicators simultaneously, or even a hybrid model with both the two models (Wang et al., 2021). Factor loadings, Cronbach's alpha, rho_A and composite reliability exceed 0.7, suggesting that this model is reliable and suitable (Yang et al., 2022).

3. Results and discussion

3.1. Characterization of Y_2O_3 NPs

Y_2O_3 NPs exhibit spherical or elliptical-shaped particles with equal sizes in TEM images (Fig. 1). Due to their large specific surface areas and small particle size, Y_2O_3 NPs are easily aggregated and coagulated in ultrapure water. The XRD pattern of Y_2O_3 NPs produce peaks at 20.5, 29.2, 33.8, 48.6, and 57.6 °2θ. The intense diffraction peaks were consistent with the standard reflections of Y_2O_3 NPs (JCPDS 43–1036), which demonstrated that the composition is pure Y_2O_3. The average diameter of NPs was 25.5 nm, according to the Debye-Scherrer formula (Ullah et al., 2020). The zeta potential of Y_2O_3 particles was 33.5 mV (ranges from ± 30 to ± 40 mV), and thus Y_2O_3 NPs have positive surface charge. The TEM results (Fig. 1) confirmed that NPs were inclined to aggregate in aqueous media, forming micron-sized aggregates that altered the effect of particle morphology and surface properties on phytotoxicity (Hazeem et al., 2016).

3.2. Effect of Y_2O_3 NP on seedling germination and growth

Germination rate, bud elongation, and root elongation are the indicators widely used for testing the phytotoxicity of chemicals (Duan et al., 2020; Ullah et al., 2020). All tests demonstrated that a high concentration of Y_2O_3 NPs led to a delay in the germination of tomato seeds but did not significantly affect the germination rate of tomato seeds after 7 days (Fig. S1). At the same time, the soluble Y^{III} appeared to only very weakly affect the germination rate of tomato seedlings. In this study, the germination time of all treatments was on the same day (Fig. S1). However, the germination rates of tomato seeds were lower than the control group at high concentrations (20–100 mg·L^{-1}). With the increasing Y_2O_3 NP stress, the germination rates of plants were not

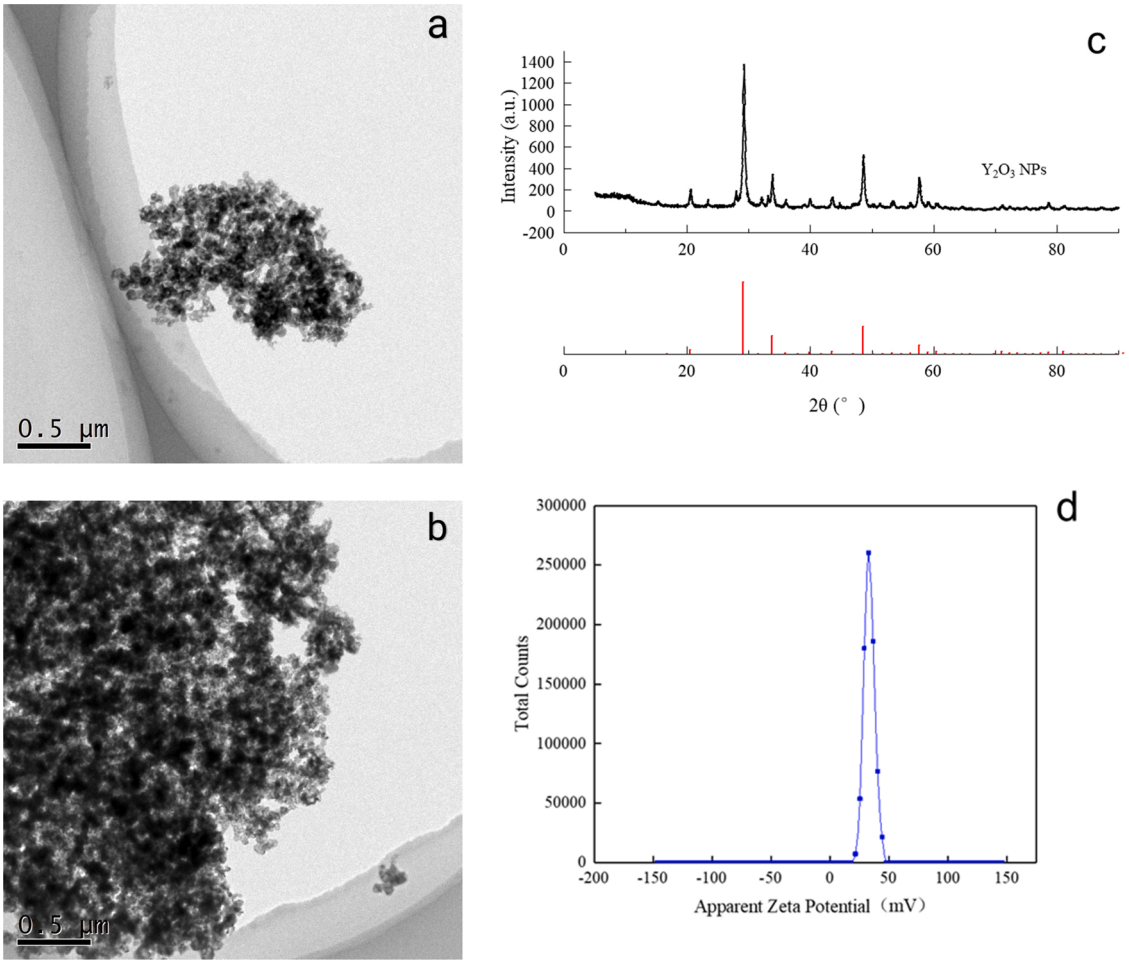

Fig. 1. TEM image (a: 50 mg·L^{-1}, b: 100 mg·L^{-1}), XRD pattern (c), and zeta potential (d) of Y_2O_3 NPs.

significantly limited with a period of 7 days. However, other morphological performance parameters (i.e., root elongation, root activity, and bud elongation) was substantially reduced in presence of Y_2O_3 NPs. After 15 days of exposure to Y_2O_3 NPs, the inhibition on bud elongation and root elongation of tomato seedlings increased significantly over the control as the NP concentration increased from 20 mg·L^{-1}, to 50 mg·L^{-1} and 100 mg·L^{-1}. Thus, the bud elongation of tomato seedlings was reduced by 48.8%, 68.8%, and 73.8%, while root elongation inhibition rates were 73.7%, 88.4% and 94.2%, and root activity was reduced by 42.0%, 66.7% and 83.6% compared with the control, respectively. Even at NP concentrations of 50 mg·L^{-1} and 100 mg·L^{-1}, seedling roots almost stopped growing on the 3rd day after germination. The effects of germination delay also have been observed for silver NPs on *Lolium perenne*, *Hordeum vulgare*, and *Oryza sativa* (Courtois et al., 2019).

The root elongation, bud elongation and root activity were reduced by 61.1%, 7.0% and 10.6% after the exposure to soluble Y^{III} at the concentration of 6.2 mg·L^{-1}. The inhibition rate of soluble Y^{III} on these effects were 0, 0.1 and 0.1 times that of Y_2O_3 NPs (100 mg·L^{-1}). Therefore, it can be concluded that it is Y_2O_3 NPs that inhibit the germination rate, bud elongation, root elongation and root activity of tomato seedlings. This was contrary to previous studies which have suggested that NPs may not significantly limit the germination rate (López-Moreno et al., 2016). In all treatments, there was a dose-dependent effect of NPs on root elongation, bud elongation, and plant growth (Fig. 2). The seed coat is an important barrier against toxic chemicals and protects the embryo from stress. The REE nano-oxides could notably influence the seed dormancy by fatty acid beta-oxidation and accelerate the mobilization of the lipid bank in glyoxysomes, which could cause a burst of reactive oxygen species and adversely affect seed germination (Ahmad et al., 2018).

3.3. Phytotoxicity of Y_2O_3 NP to tomato

Chlorophyll is a major green photosynthetic pigment that accounts for the ability to absorb sunlight and the intensity of photosynthesis. In the present study, we found an inhibition effect of Y_2O_3 NPs on chlorophyll contents in tomato seedlings, and the degree of inhibition was in proportion to the concentrations of Y_2O_3 NPs (Fig. 3). The chlorophyll content did not show a significant difference related to the concentration of soluble Y^{III} and low concentrations of Y_2O_3 NPs (1 and 5 mg·L^{-1}). However, with the higher concentration of NPs the chlorophyll content was reduced by 25.3% (20 mg·L^{-1}), 34.2% (50 mg·L^{-1}) and 46.1% (100 mg·L^{-1}), respectively, compared to control group.

The proline content in tomato seedlings grown in Y_2O_3 NP treatments was 1.1–2.5 times higher than that of the control group for all treatments, and it increased with elevated Y_2O_3 NP concentration. Besides, the proline content was 1.7 times that of the control group after exposure to soluble Y^{III}. In comparison with the control treatment, a positive correlation was seen between MDA in tomato seedlings and the concentration of Y_2O_3 NPs across all treatments (Fig. 3). After exposure for 15 days, the content of MDA in tomato seedlings treated with Y_2O_3 NPs and soluble Y^{III} ranged from 1.1 to 2.4 times compared with the control, which indicated that Y_2O_3 NPs and soluble Y^{III} induced plant membrane lipid peroxidation and cause a certain degree of damage to the plant membrane system. Among that, two exposure concentrations of Y_2O_3 NPs (50 mg·L^{-1} and 100 mg·L^{-1}) inhibited SOD after 15 days of

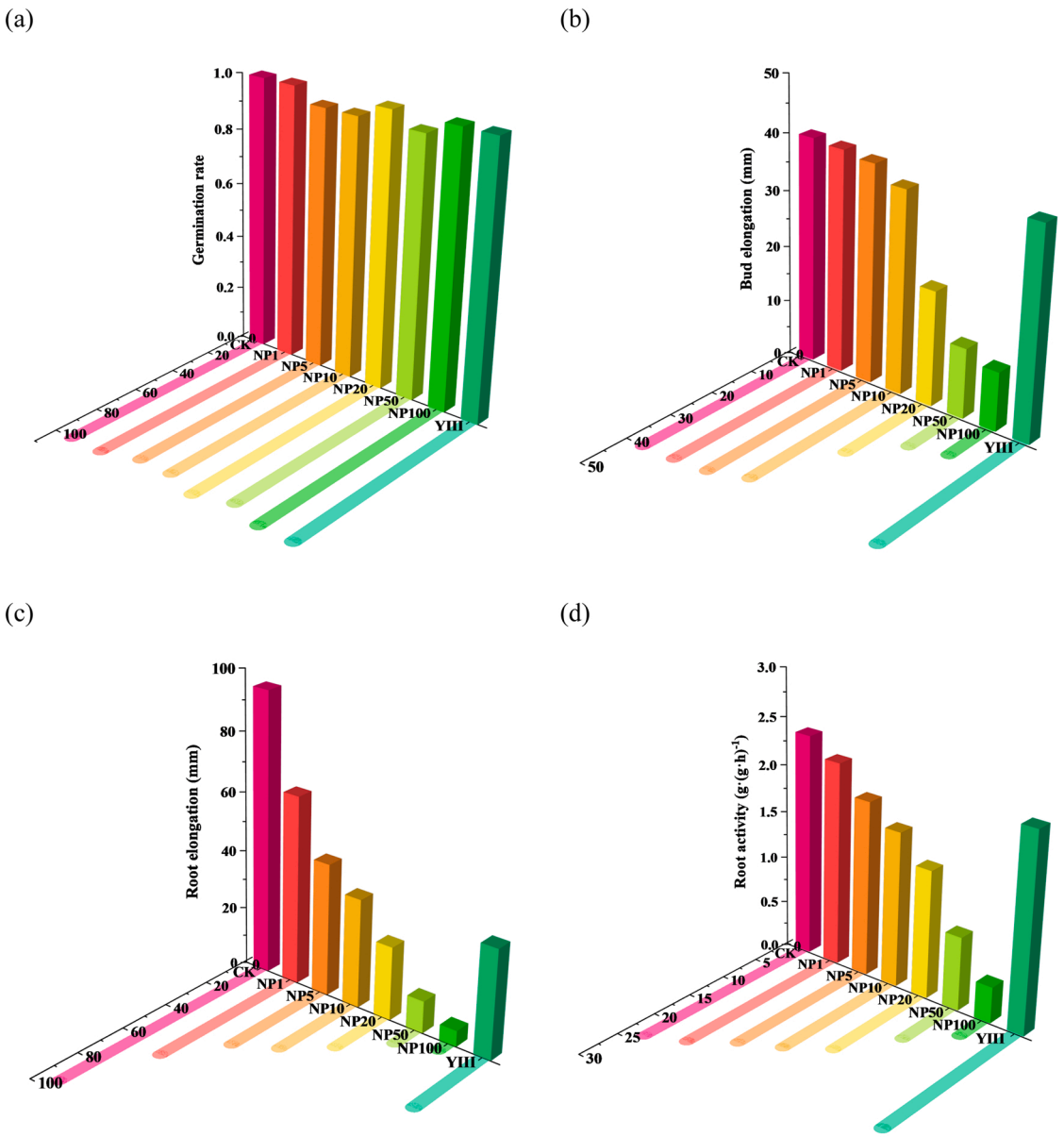

Fig. 2. Effects of Y_2O_3 NPs and soluble Y^{III} on the germination rate (a), root elongation (b), bud elongation (c) and root activity (d) of tomato seedlings. CK represents the control group.

exposure with a reduction of 71.0% and 60.3% compared to the control, respectively. No significant change occurred in the 1.0 mg·L^{-1} Y_2O_3 NPs treatment. The SOD effect was proportional to the Y_2O_3 concentrations of the solutions. The inhibiting effect of Y_2O_3 NPs on seedlings resulted in toxicity of NPs, which damaged the antioxidant capacity and membrane system in the tomato seedlings.

The soluble protein content in tomato seedlings was negatively correlated with the exposure concentrations of the NPs. When exposed to 1–100 mg·L^{-1} Y_2O_3 NPs and soluble Y^{III} for 15 days, the reduction rates of protein content in seedlings were 5.7–78.6% and 27.9%, respectively, compared to the control group (Fig. 3). In conclusion, Y_2O_3 NPs had a significant inhibition effect on tomato soluble protein. The soluble protein content in plants treated with Y_2O_3 NPs above 20 mg·L^{-1} was lower than in the treatment with soluble Y^{III}, which revealed that Y_2O_3 NPs above 20 mg·L^{-1} had a greater inhibition effect on tomato seedlings than soluble Y^{III}.

When plants are stressed, there is an excessive accumulation of reactive oxygen species (ROS) in the plant, which causes lipid peroxidation, osmotic changes, protein oxidation and impaired metabolism (Ahluwalia et al., 2021). MDA and proline are the main cytotoxic product of membrane lipid peroxidation and a potent antioxidant, respectively, reflecting the extent of damage in plants (Courtois et al., 2019). Y_2O_3 NPs have a prominent effect on lipid peroxidation and physiological indicators, expressed in the increased concentrations of proline and MDA with the increased NP concentrations. SOD and soluble protein content showed opposite trends. The inhibition rate of soluble Y^{III} on chlorophyll content, soluble protein content and SOD were 1.1%, 6.1% and 1.8%, while the concentrations of proline and MDA at the treatment with soluble Y^{III} were higher than the control group. The change in SOD, MDA, proline and soluble protein revealed that the ROS accumulation caused by NPs had exceeded the elimination ability of antioxidative enzymes (Lin et al., 2020). In contrast, SOD in the shoot was higher than in the control group when cucumber seedlings were exposed to CeO_2 NPs (Akanbi-Gada et al., 2019; Xie et al., 2022). Therefore, the SOD change in plants was affected by the phytotoxicity of NPs. Soluble Y^{III} had a certain toxic effect on tomato seedlings, but the negative effect of Y_2O_3 NPs was higher than soluble Y^{III} due to their nanotoxicity (Yu et al., 2020).

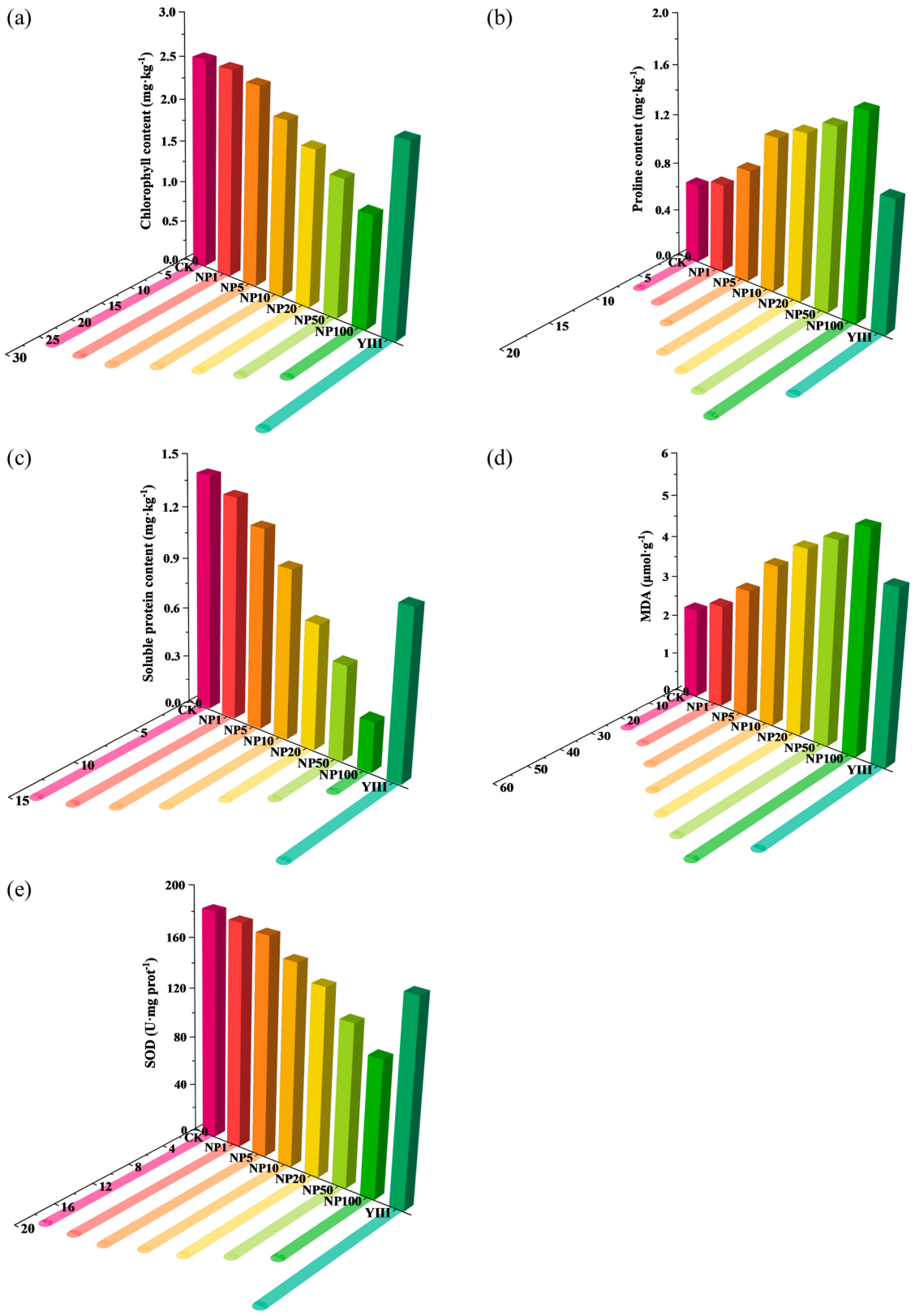

Fig. 3. Effects of Y_2O_3 NPs and soluble Y^{III} on chlorophyll content(a), proline (b), MDA (c), SOD (d) and soluble protein content (e) of tomato seedlings. CK represents the control group.

Lipid peroxidation is seen in plants exposed to abiotic stresses, such as from metal-based NPs, due to over-generation of ROS. To protect cells from the toxic effects of ROS, plants scavenge damage-induced ROS through various defense mechanisms, of which the enzyme-antioxidant system is one of the protective mechanisms (Hou et al., 2017). In addition, proline regulates ROS in cells by acting in synergy with antioxidant enzymes and non-enzymatic peroxidation systems (Courtois et al., 2019). The changes in soluble protein, antioxidative enzymes (i.e.,

SOD), low molecular weight antioxidants (i.e., proline) and non-enzymatic components (i.e., MDA) reflected the oxidative damage resulting from nano metal oxides on cell membrane integrity (Siddiqi and Husen, 2017). Other NPs, such as NiO NPs (Faisal et al., 2013), $CoFeO_4$ NPs (López-Moreno et al., 2016) and CeO_2 NPs (Li et al., 2019), also affected oxidative stress and protein synthesis in plants.

3.4. Y_2O_3 NP uptake and translocation in tomato

The yttrium concentration in different plant parts was measured to specify the translocation of Y_2O_3 NPs. The bioaccumulation factor (BAF) is applied to describe the degree to which substances are accumulated into plant tissues from the growth medium, which is measured as the ratio of contaminant concentrations in plant tissue to the growing medium (Bolan et al., 2013; Guo et al., 2021). Besides, the translocation factor (TF) is an important tool to evaluate the accumulation and translocation of chemicals in plants, which is defined as the ratio of contaminant concentrations in shoots to the roots (C_{shoot} / C_{root}) (Malandrakis et al., 2021). The results showed that with the elevated NP concentration in the growing medium, the yttrium concentrations in seedlings increased. The yttrium contents in the shoots were 3.0, 6.7, 39.9, 57.0, 67.5, and 212 times higher than the control, respectively, while those in roots under the various treatments were 185, 533, 700, 1610, 1910, and 2920 times the control (Fig. 4). The BAF values in the shoot were less than 1, while the BAF values in root were greater than 1 under the same treatment. The trend of TF elucidates that a continuous decline in BAF value was observed from 1 to 50 $mg{\cdot}L^{-1}$, and with all TF values less than 1. The observation of BAF and TF exhibited that the Y_2O_3 NPs would be more liable to bioaccumulate in roots than shoot.

The concentration-dependent uptake of Y_2O_3 NPs by tomato shoot was linear and was well fitted by the analogous Michaelis–Menten model ($R^2 > 93.4\%$, $P < 0.05$) with a V_{max} of 1.0 $mg{\cdot}(kg{\cdot}h)^{-1}$ and K_t of 2.9 (Fig. 4). Unlike the shoot, the uptake process of NPs by root was nonlinear, and the calculated V_{max} and K_t were 113.5 $mg{\cdot}(kg{\cdot}h)^{-1}$ and 31.2, respectively. The results are in line with the translocation of NPs in roots. After the exposure to Y_2O_3 NPs, Y_2O_3 NPs proved to have a concentration-dependent inhibition on the biomass of shoot and root ($P < 0.05$) (Fig. 4). The shoot biomass was reduced by 0.2–6.3% across all levels of Y_2O_3 NPs, while the reduction for roots ranged between 1.0% and 11.3%. Thus, there was a stronger inhibition of Y_2O_3 NPs on root biomass than shoot biomass. The root is the primary entrance of NPs in the plant, with absorption of NPs on the epidermis and exodermis (Abbas et al., 2019; Siddiqi and Husen, 2017). The damage to the cell membrane in the root by accumulated NPs would block water and nutrient transport from root to shoot, such as the levels and distribution of N, P and K in plant tissues, which leads to a negative effect on seedling growth and biomass (Abbas et al., 2020b; Antoniadis et al., 2017; Tombuloglu et al., 2020).

3.5. Translocation mechanism

To better understand the translocation of Y_2O_3 NPs to tomato seedlings, Y_2O_3 NPs in the leaves of tomato seedlings were determined by TEM (Fig. 5). EDS (Fig. 5a) demonstrates that the black granular substances in the cells has the highest Y and O concentrations, demonstrating that these are the Y_2O_3 NPs. There was no NPs in leaf cells of tomato seedlings of the control group, which had intact cell structures and morphology. However, Y_2O_3 NPs were found in the intercellular

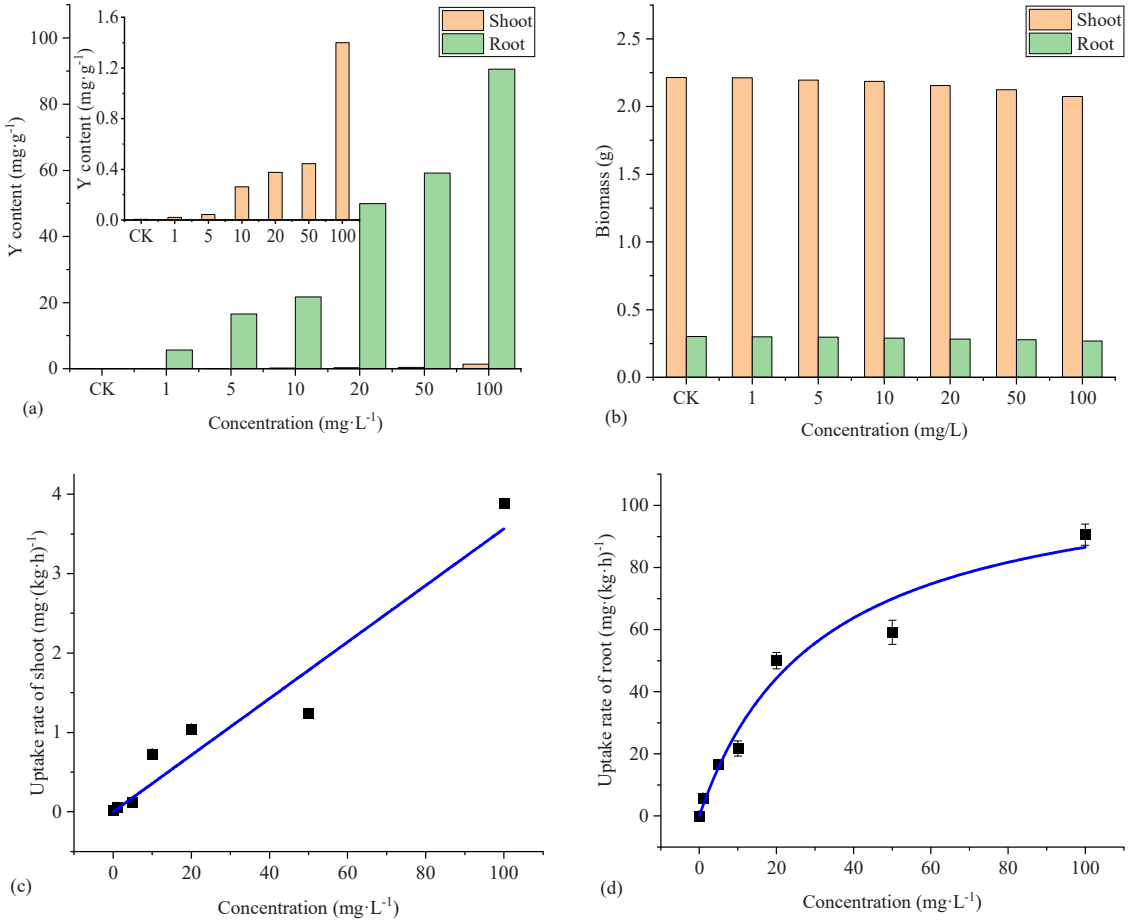

Fig. 4. Effects of Y_2O_3 NPs on the yttrium concentration (a), biomass (b) of shoot and root in tomato seedling. The concentration-dependent uptake of Y_2O_3 NPs in the shoot (c) and root (d). CK represents the control group. The line (c) and curve (d) represent the fitting of the Michaelis-Menten equation.

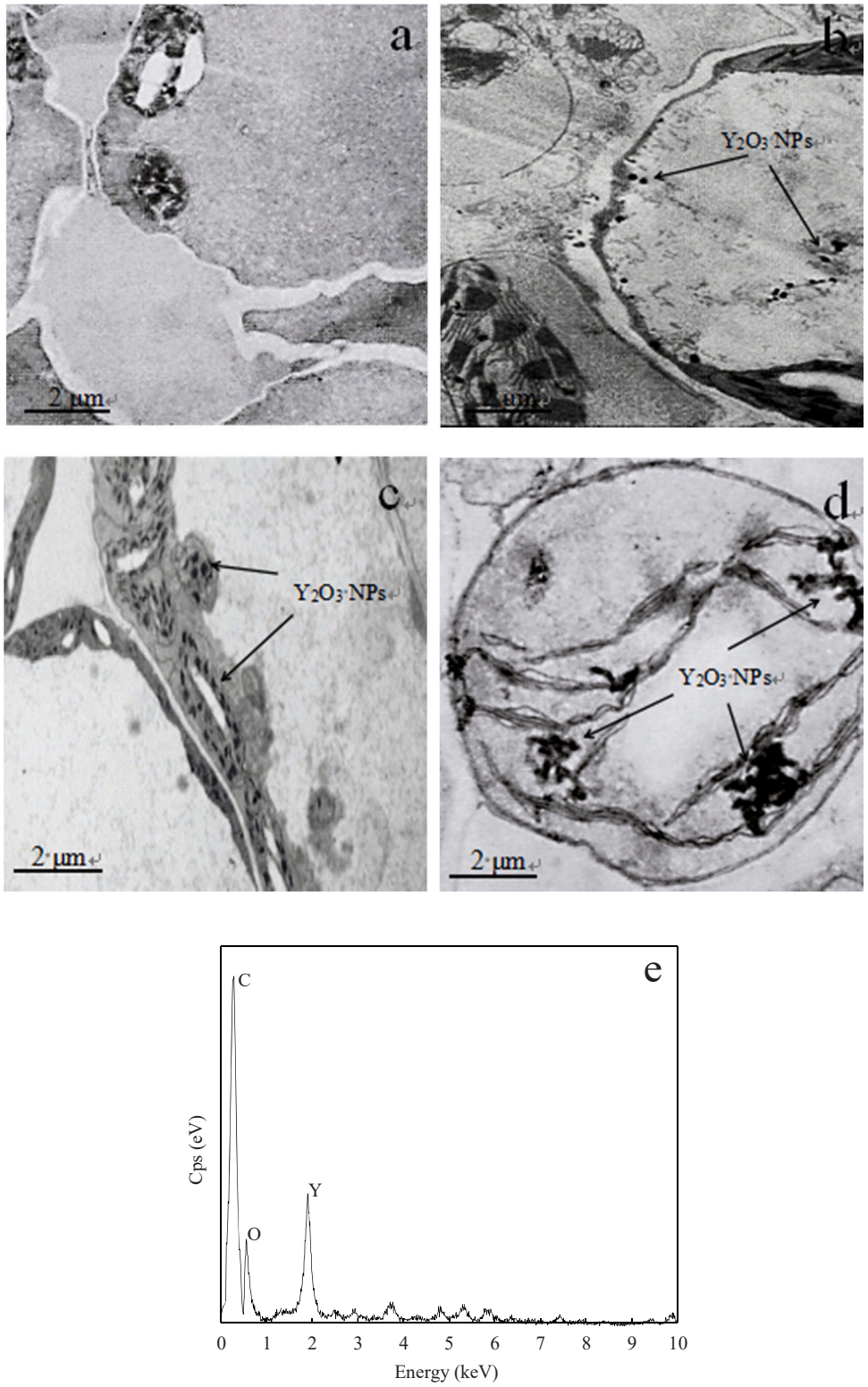

Fig. 5. TEM of tomato mesophyll cells under the control group (a) and Y_2O_3 NPs treatment (b-d). EDS of black granules in leaf cells of tomato seedlings (e).

space, cell wall and the chloroplast of tomato leaf samples in the treatment of 100 mg·L^{-1} NPs (Fig. 5b, c, d), which reflected that Y_2O_3 NPs could penetrate through the epidermis through the cortex as the apoplastic path. In addition, the observed vesicle-like structures illustrated that endocytosis was a translocation pathway of Y_2O_3 NPs to tomato seedlings (Fig. 5c). The entrance of NPs into plants is regulated by their particular barrier, which is mainly achieved by altering the solubility and other properties of the polymer as polysaccharides and pectin in the cell wall (Fincheira et al., 2020). Lv et al. (2019) have observed that NPs larger than 20 nm could enter the intercellular space, but only NPs smaller than 20 nm could cross the cell wall. NPs may enter the intercellular space or even the xylem through damaged cell walls, enlarged pore diameters, or damaged roots caused by underground herbivores and mechanical diseases (Ullah et al., 2020). Hydroponic experiments

have many advantages. For example, in hydroponic system, it is easy to control plant growth conditions (e.g., temperature, water flow rate and volume, nutrients, relative humidity and light duration) and less disturbance by external environmental factors, which also can prevent diseases from soil and reuse of water and nutrients (Lee and Lee, 2015). Therefore, the hydroponic experiment is a common method to evaluate the toxicity of chemicals (Lee and Lee, 2015). At the same time, this method does not mimic field conditions and may overestimate the phytotoxicity of NPs (García-Gómez et al., 2017). Fig. 6.

3.6. A model for the effect of Y_2O_3 NPs on the growth of tomato seedlings

NPs may affect many morphological, physiological and biochemical functions during the germination and growth of seedlings (Abbas et al., 2020a). PLS-SEM was used to quantify the relationship between NPs, physiological and biochemical indicators, and seedling biomass using Smart PLS 3.0 software (Aboelmaged, 2018). All factor loadings of the measurement model were considered suitable because these loadings exceeded the threshold value of 0.7. Measurement reliability indicators, Cronbach's alpha, rho_A and composite reliability surpassed 0.7, suggesting adequate internal reliability of variables in this model (Wang et al., 2021). Moreover, the average variance extracted (AVE), the square of inter-construct correlations and variances loadings were more significant than the required threshold, which revealed a satisfactory convergent and discriminative validity of the model (Aboelmaged, 2018; Henseler et al., 2016). The model fitted and predicted the data well, with a high R^2 of all variances and predictive relevance (Q^2). The loadings of measurement and structural models were significant ($P < 0.01$), and the T-test values greater than 2.0 confirmed the significance.

The PLS-SEM model explained 97.9% of the variation in seedling biomass. The results showed that the concentration of Y_2O_3 NPs in nutrient solution significantly affects the distribution of NPs in tomato seedlings (e.g., content in shoots and roots) with a path coefficient of 0.9. The physiological and biochemical indexes of seedlings, including the chlorophyll, proline, MDA, SOD, soluble protein, and root activity, were significantly influenced by NPs (path coefficient of −0.9), with a whole indicator loading of 1.0. These indicators had a significant positive effect on the biomass of seedlings in shoot and root with a coefficient of 1.0. The concentration of NPs significantly affected plants' morphology, physiology and biomass of shoot and root in plant. Hence, high concentration of NPs led to low biomass of plants.

Exposure to REONPs present a stress factor affecting plant nutrient and water absorption and growth, leading to differences in biomass (Du et al., 2019). The root surface is negatively charged because of specific organic acid functional groups and mucus secreted by the root hairs.

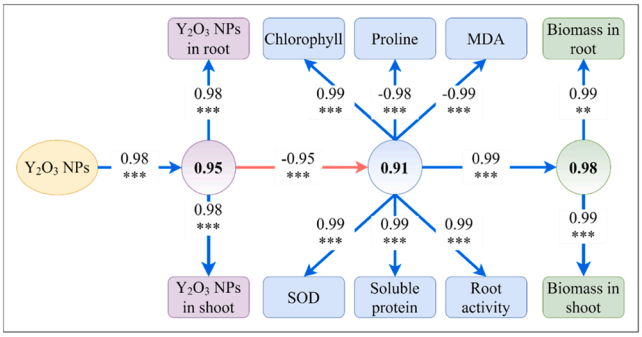

Fig. 6. The relationship between NP concentration, physiological and morphological indicators, and biomass of plants. The circles and rectangles represent latent variables and manifest variables, respectively. The arrows represent the cause-total effect of the four variables with the path coefficient. The solid red and dotted blue lines represent negative and positive correlations, respectively. All path coefficients are significant at the 99.9% confidence level.

Therefore, the root tends to adsorb and accumulate the positively charged NPs (Abbas et al., 2021). After that, NPs must pass through a series of physiological barriers and translocate from root to the shoot through the xylem, resulting in the changes in physiological, biochemical indicators and biomass of shoot and root (Abbas et al., 2020a; Lv et al., 2019). The transformation and uptake of REONPs on plants depend on the exposure concentration of NPs. It has been demonstrated that some plants' growth was promoted at low concentrations of REONPs and inhibited at a higher concentration (Gong et al., 2019). Moreover, microorganisms and root exudates in the rhizosphere are the critical factors contributing to the uptake and translocation pathway of REONPs to plants (Hong et al., 2016). Herein, reducing the concentration and bioavailability of REONPs in soils and water was the primary way to control NPs in plants.

The phytotoxicity of NPs on plants was determined by the characteristics of NPs, such as type, particle size and shape (Yang et al., 2017a, 2017b). For instance, the exposure to Fe_3O_4 NPs and TiO_2 NPs induced stronger metabolic reprogramming in maize leaves and roots than SiO_2 NPs (Zhao et al., 2019). AuNPs were detected in tobacco (*Nicotiana xanthi*) at 3.5 nm spheres, but AuNPs in the form of 18 nm remained aggregated on the outer surface of the root (Sabo-Attwood et al., 2012). The rod-like CeO_2 NPs have the largest amount of Ce in hydroponic cucumber plants and the highest chemical reactivity compared with octahedral, cubic and irregularly shaped CeO_2 NPs (Zhang et al., 2017). Besides, plant species, growth medium and growth stage, microorganisms and exudates in the rhizosphere significantly influenced the phytotoxicity of NPs (Yang et al., 2017a, 2017b). ZnO NPs had a stronger effect on oxidative stress of legumes in acidic soil than in calcareous soils, while the opposite was true for tomatoes (García-Gómez et al., 2017). There were no significant changes and suddenly reduced chlorophyll contents in barley leaves after the exposure to CuO NPs for 10 d and 20 d, respectively (Shaw et al., 2014). The addition of root exudates inhibited the growth rate of maize seedlings and increased the phytotoxicity of CuO NPs (Shang et al., 2019).

4. Conclusion

This study aimed to elucidate the morphological, physiological, and phytotoxic effects of Y_2O_3 NPs (mean size 25.5 nm) on the germination and growth of tomato seedlings. The finding revealed that most Y_2O_3 NPs treatments (> 10 mg·L^{-1}) and soluble Y^{III} delayed the germination of seeds, which inhibited the bud elongation, root elongation and root activity compared with the control. Similar results were observed for the effect of Y_2O_3 NPs on physiological indicators and membrane lipid peroxidation. Compared with soluble Y^{III}, all Y_2O_3 NPs treatments had greater phytotoxic effect on tomato seedlings. The BAF values for shoots and roots were less than 1 and greater than 1, respectively. The shoot biomass was reduced by 0.2–6.3% across all levels of Y_2O_3 NPs, while the reduction for roots ranged between 1.0% and 11.3%. The bioaccumulation factor, translocation factor, uptake process and biomass showed the translocation of NPs from root to shoot, and NPs tended to bioaccumulate in roots. Y_2O_3 NPs entered the cell wall through endocytosis and were present in the intercellular spaces and cytoplasm of tomato seedling mesophyll cells. These results contributes to understanding of the translocation mechanism of Y_2O_3 NPs and the interaction between Y_2O_3 NPs and plants. Besides, the result of PLS-SEM confirmed the phytotoxic impact of Y_2O_3 NPs on the tomato seedlings under all treatments. Here, the translocation of Y_2O_3 NPs was also affected by characteristics of NPs, plant growth and exposure medium. This study is conducive to understanding and evaluating the influences of REONPs on the physiological uptake, translocation and phytotoxicity in plants. At the same time, it provides a basis for assessing the ecological and health risks caused by NPs through the food chain.

CRediT authorship contribution statement

Xueping Wang: Investigation, Methodology, Formal analysis, Visualization, Writing – original draft. **Xiaojie Liu**: Validation, Methodology, Visualization, Writing – original draft. **Lingqing Wang**: Conceptualization, Methodology, Writing – review & editing, Supervision. **Xiao Yang**: Investigation, Validation. **Jun Yang**: Methodology, Validation. **Xiulan Yan**: Investigation, Validation. **Tao Liang**: Formal analysis, Data curation, Writing – review & editing. **Hans Chr. Bruun Hansen**: Validation, Writing – review & editing. **Balal Yousaf**: Methodology, Validation, Writing – review & editing. **Sabry M. Shaheen**: Methodology, Formal analysis, Writing – review & editing. **Nanthi Bolan**: Validation, Writing – review & editing. **Jörg Rinklebe**: Conceptualization, Validation, Supervision, Writing – review & editing.

Declaration of Competing Interest

The authors declare that they have no known competing financial interests or personal relationships that could have appeared to influence the work reported in this paper.

Data availability

Data will be made available on request.

Acknowledgments

This work was sponsored by the National Natural Science Foundation of China (42173064). Dr. Lingqing Wang is thankful to the Alexander von Humboldt Foundation for the experienced researcher's fellowships in Prof. Dr. Jörg Rinklebe's laboratory at the University of Wuppertal, Germany.

Appendix A. Supporting information

Supplementary data associated with this article can be found in the online version at doi:10.1016/j.ecoenv.2022.113939.

References

Abbas, Q., Liu, G., Yousaf, B., Ali, M.U., Ullah, H., Ahmed, R., 2019. Effects of biochar on uptake, acquisition and translocation of silver nanoparticles in rice (*Oryza sativa L.*) in relation to growth, photosynthetic traits and nutrients displacement. Environ. Pollut. 250, 728–736.

Abbas, Q., Yousaf, B., Amina, Ali, M.U., Munir, M.A.M., El-Naggar, A., Rinklebe, J., Naushad, M., 2020a. Transformation pathways and fate of engineered nanoparticles (ENPs) in distinct interactive environmental compartments: a review. Environ. Int. 138, 105646.

Abbas, Q., Yousaf, B., Mujtaba Munir, M.A., Cheema, A.I., Hussain, I., Rinklebe, J., 2021. Biochar-mediated transformation of titanium dioxide nanoparticles concerning TiO_2NPs-biochar interactions, plant traits and tissue accumulation to cell translocation. Environ. Pollut. 270, 116077.

Abbas, Q., Yousaf, B., Ullah, H., Ali, M.U., Zia-ur-Rehman, M., Rizwan, M., Rinklebe, J., 2020b. Biochar-induced immobilization and transformation of silver-nanoparticles affect growth, intracellular-radicles generation and nutrients assimilation by reducing oxidative stress in maize. J. Hazard. Mater. 390, 121976.

Aboelmaged, M., 2018. The drivers of sustainable manufacturing practices in Egyptian SMEs and their impact on competitive capabilities: a PLS-SEM model. J. Clean. Prod. 175, 207–221.

Agathokleous, E., Kitao, M., Calabrese, E.J., 2018. The rare earth element (REE) lanthanum (La) induces hormesis in plants. Environ. Pollut. 238, 1044–1047.

Ahluwalia, O., Singh, P.C., Bhatia, R., 2021. A review on drought stress in plants: Implications, mitigation and the role of plant growth promoting rhizobacteria. Resour. Environ. Sustain. 5, 100032.

Ahmad, H.R., Zia-ur-Rehman, M., Sohail, M.I., Anwar ul Haq, M., Khalid, H., Ayub, M.A., Ishaq, G., 2018. Effects of rare earth oxide nanoparticles on plants. In: Nanomaterials in Plants, Algae, and Microorganisms. Elsevier, pp. 239–275.

Akanbi-Gada, M.A., Ogunkunle, C.O., Vishwakarma, V., Viswanathan, K., Fatoba, P.O., 2019. Phytotoxicity of nano-zinc oxide to tomato plant (*Solanum lycopersicum L.*): Zn uptake, stress enzymes response and influence on non-enzymatic antioxidants in fruits. Environ. Technol. Innov. 14, 100325.

Antoniadis, V., Levizou, E., Shaheen, S.M., Ok, Y.S., Sebastian, A., Baum, C., Prasad, M.N. V., Wenzel, W.W., Rinklebe, J., 2017. Trace elements in the soil-plant interface: phytoavailability, translocation, and phytoremediation–a review. Earth Sci. Rev. 171, 621–645.

Balaram, V., 2019. Rare earth elements: a review of applications, occurrence, exploration, analysis, recycling, and environmental impact. Geosci. Front. 10, 1285–1303.

Bolan, N., Mahimairaja, S., Kunhikrishnan, A., Choppala, G., 2013. Phosphorus–arsenic interactions in variable-charge soils in relation to arsenic mobility and bioavailability. Sci. Total Environ. 463–464, 1154–1162.

Chen, Y., Sanchez, C., Yue, Y., de Almeida, M., González, J.M., Parkinson, D.Y., Liang, H., 2016. Observation of yttrium oxide nanoparticles in cabbage (*Brassica oleracea*) through dual energy K-edge subtraction imaging. J. Nanobiotechnol. 14, 23.

Courtois, P., Rorat, A., Lemiere, S., Guyoneaud, R., Attard, E., Levard, C., Vandenbulcke, F., 2019. Ecotoxicology of silver nanoparticles and their derivatives introduced in soil with or without sewage sludge: a review of effects on microorganisms, plants and animals. Environ. Pollut. 253, 578–598.

Dong, C., Jiao, C., Xie, C., Liu, Y., Luo, W., Fan, S., Ma, Y., He, X., Lin, A., Zhang, Z., 2021. Effects of ceria nanoparticles and CeCl3 on growth, physiological and biochemical parameters of corn (*Zea mays*) plants grown in soil. NanoImpact 22, 100311.

Dragun, Z., Filipović Marijić, V., Krasnići, N., Ramani, S., Valić, D., Rebok, K., Kostov, V., Jordanova, M., Erk, M., 2017. Malondialdehyde concentrations in the intestine and gills of Vardar chub (*Squalius vardarensis Karaman*) as indicator of lipid peroxidation. Environ. Sci. Pollut. Res. 24, 16917–16926.

Du, W., Yang, J., Peng, Q., Liang, X., Mao, H., 2019. Comparison study of zinc nanoparticles and zinc sulphate on wheat growth: from toxicity and zinc biofortification. Chemosphere 227, 109–116.

Duan, D., Tong, J., Xu, Q., Dai, L., Ye, J., Wu, H., Xu, C., Shi, J., 2020. Regulation mechanisms of humic acid on Pb stress in tea plant (*Camellia sinensis L.*). Environ. Pollut. 267, 115546.

Faisal, M., Saquib, Q., Alatar, A.A., Al-Khedhairy, A.A., Hegazy, A.K., Musarrat, J., 2013. Phytotoxic hazards of NiO-nanoparticles in tomato: a study on mechanism of cell death. J. Hazard. Mater. 250–251, 318–332.

Fincheira, P., Tortella, G., Duran, N., Seabra, A.B., Rubilar, O., 2020. Current applications of nanotechnology to develop plant growth inducer agents as an innovation strategy. Crit. Rev. Biotechnol. 40, 15–30.

García-Gómez, C., Obrador, A., González, D., Babín, M., Fernández, M.D., 2017. Comparative effect of ZnO NPs, ZnO bulk and $ZnSO_4$ in the antioxidant defences of two plant species growing in two agricultural soils under greenhouse conditions. Sci. Total Environ. 589, 11–24.

Gong, C., Wang, L., Li, X., Wang, H., Jiang, Y., Wang, W., 2019. Responses of seed germination and shoot metabolic profiles of maize (*Zea mays L.*) to Y_2O_3 nanoparticle stress. RSC Adv. 9, 27720–27731.

Guo, W., Dai, Y., Chu, X., Cui, S., Sun, Y., Li, Y.F., Jia, H., 2021. Assessment bioaccumulation factor (BAF) of methyl siloxanes in crucian carp (*Carassius auratus*) around a siloxane production factory. Ecotoxicol. Environ. Saf. 213, 111983.

Hair, J.F., Risher, J.J., Sarstedt, M., Ringle, C.M., 2019. When to use and how to report the results of PLS-SEM. Eur. Bus. Rev. 31, 2–24.

Hazeem, L.J., Bououdina, M., Rashdan, S., Brunet, L., Slomianny, C., Boukherroub, R., 2016. Cumulative effect of zinc oxide and titanium oxide nanoparticles on growth and chlorophyll a content of Picochlorum sp. Environ. Sci. Pollut. Res. 23, 2821–2830.

Henseler, J., Hubona, G., Ray, P.A., 2016. Using PLS path modeling in new technology research: updated guidelines. Ind. Manag. Data Syst. 116, 2–20.

Hong, J., Wang, L., Sun, Y., Zhao, L., Niu, G., Tan, W., Rico, C.M., Peralta-Videa, J.R., Gardea-Torresdey, J.L., 2016. Foliar applied nanoscale and microscale CeO2 and CuO alter cucumber (*Cucumis sativus*) fruit quality. Sci. Total Environ. 563–564, 904–911.

Hou, J., Wang, X.X., Hayat, T., Wang, X.K., 2017. Ecotoxicological effects and mechanism of CuO nanoparticles to individual organisms. Environ. Pollut. 221, 209–217.

Iftikhar, A., Ali, S., Yasmeen, T., Arif, M.S., Zubair, M., Rizwan, M., Alhaithloul, H.A.S., Alayafi, A.A.M., Soliman, M.H., 2019. Effect of gibberellic acid on growth, photosynthesis and antioxidant defense system of wheat under zinc oxide nanoparticle stress. Environ. Pollut. 254, 113109.

Khanna, K., Kohli, S.K., Handa, N., Kaur, H., Ohri, P., Bhardwaj, R., Yousaf, B., Rinklebe, J., Ahmad, P., 2021. Enthralling the impact of engineered nanoparticles on soil microbiome: a concentric approach towards environmental risks and cogitation. Ecotoxicol. Environ. Saf. 222, 112459.

Lee, S., Lee, J., 2015. Beneficial bacteria and fungi in hydroponic systems: types and characteristics of hydroponic food production methods. Sci. Hortic. 195, 206–215.

Lei, P., Xu, Z., Liang, J., Luo, X., Zhang, Y., Feng, X., Xu, H., 2016. Poly(γ-glutamic acid) enhanced tolerance to salt stress by promoting proline accumulation in Brassica napus L. Plant Growth Regul. 78, 233–241.

Li, J., Tappero, R.V., Acerbo, A.S., Yan, H., Chu, Y., Lowry, G.V., Unrine, J.M., 2019. Effect of CeO_2 nanomaterial surface functional groups on tissue and subcellular distribution of Ce in tomato (*Solanum lycopersicum*). Environ. Sci. Nano 6, 273–285.

Lichtenthaler, H.K., 1987. Chlorophylls and carotenoids: pigments of photosynthetic biomembranes. In: Methods in Enzymology, Plant Cell Membranes. Academic Press, pp. 350–382.

Lin, F., Sun, J., Liu, N., Zhu, L., 2020. Phytotoxicity and metabolic responses induced by tetrachlorobiphenyl and its hydroxylated and methoxylated derivatives in rice (*Oryza sative L.*). Environ. Int. 139, 105695.

López-Moreno, M.L., Avilés, L.L., Pérez, N.G., Irizarry, B.Á., Perales, O., Cedeno-Mattei, Y., Román, F., 2016. Effect of cobalt ferrite ($CoFe_2O_4$) nanoparticles on the growth and development of *Lycopersicon lycopersicum* (tomato plants). Sci. Total Environ. 550, 45–52.

Lv, J., Christie, P., Zhang, S., 2019. Uptake, translocation, and transformation of metal-based nanoparticles in plants: recent advances and methodological challenges. Environ. Sci. Nano 6, 41–59.
Ma, Y., Kuang, L., He, X., Bai, W., Ding, Y., Zhang, Z., Zhao, Y., Chai, Z., 2010. Effects of rare earth oxide nanoparticles on root elongation of plants. Chemosphere 78, 273–279.
Malandrakis, A.A., Kavroulakis, N., Avramidou, M., Papadopoulou, K.K., Tsaniklidis, G., Chrysikopoulos, C.V., 2021. Metal nanoparticles: phytotoxicity on tomato and effect on symbiosis with the Fusarium solani FsK strain. Sci. Total Environ. 787, 147606.
Mihajlovic, J., Stärk, H.J., Rinklebe, J., 2017. Rare earth elements and their release dynamics under pre-definite redox conditions in a floodplain soil. Chemosphere 181, 313–319.
Ovelar, R.L., Fernández-Boy, M.E., Knicker, H., 2021. Characterization of the residue (endocarp) of Acrocomia aculeate and its biochars as potential peat substitute in tomato cultivation (No. EGU21–3224). Presented at the EGU21, Copernicus Meetings.
Peijnenburg, W., Praetorius, A., Scott-Fordsmand, J., Cornelis, G., 2016. Fate assessment of engineered nanoparticles in solids dominated media – current insights and the way forward. Environ. Pollut. 218, 1365–1369.
Qi, L., Ge, Y., Xia, T., He, J.Z., Shen, C., Wang, J., Liu, Y.J., 2019. Rare earth oxide nanoparticles promote soil microbial antibiotic resistance by selectively enriching antibiotic resistance genes. Environ. Sci. Nano 6, 456–466.
Rajput, V., Minkina, T., Fedorenko, A., Sushkova, S., Mandzhieva, S., Lysenko, V., Duplii, N., Fedorenko, G., Dvadnenko, K., Ghazaryan, K., 2018. Toxicity of copper oxide nanoparticles on spring barley (*Hordeum sativum distichum*). Sci. Total Environ. 645, 1103–1113.
Sabo-Attwood, T., Unrine, J.M., Stone, J.W., Murphy, C.J., Ghoshroy, S., Blom, D., Bertsch, P.M., Newman, L.A., 2012. Uptake, distribution and toxicity of gold nanoparticles in tobacco (*Nicotiana xanthi*) seedlings. Nanotoxicology 6, 353–360.
Selvaraj, V., Bodapati, S., Murray, E., Rice, K.M., Winston, N., Shokuhfar, T., Zhao, Y., Blough, E., 2014. Cytotoxicity and genotoxicity caused by yttrium oxide nanoparticles in HEK293 cells. Int. J. Nanomed. 9, 1379–1391.
Shang, H., Guo, H., Ma, C., Li, C., Chefetz, B., Polubesova, T., Xing, B., 2019. Maize (*Zea mays L.*) root exudates modify the surface chemistry of CuO nanoparticles: altered aggregation, dissolution and toxicity. Sci. Total Environ. 690, 502–510.
Shaw, A.K., Ghosh, S., Kalaji, H.M., Bosa, K., Brestic, M., Zivcak, M., Hossain, Z., 2014. Nano-CuO stress induced modulation of antioxidative defense and photosynthetic performance of Syrian barley (*Hordeum vulgare L.*). Environ. Exp. Bot. 102, 37–47.
Siddiqi, K.S., Husen, A., 2017. Plant response to engineered metal oxide nanoparticles. Nanoscale Res. Lett. 12, 92.
Spielman-Sun, E., Avellan, A., Bland, G.D., Tappero, R.V., Acerbo, A.S., Unrine, J.M., Giraldo, J.P., Lowry, G.V., 2019. Nanoparticle surface charge influences translocation and leaf distribution in vascular plants with contrasting anatomy. Environ. Sci. Nano 6, 2508–2519.
Tian, S., Liang, T., Li, K., Wang, L., 2018. Source and path identification of metals pollution in a mining area by PMF and rare earth element patterns in road dust. Sci. Total Environ. 633, 958–966.
Tombuloglu, H., Slimani, Y., AlShammari, T.M., Bargouti, M., Ozdemir, M., Tombuloglu, G., Akhtar, S., Sabit, H., Hakeem, K.R., Almessiere, M., Ercan, I., Baykal, A., 2020. Uptake, translocation, and physiological effects of hematite (α-Fe_2O_3) nanoparticles in barley (*Hordeum vulgare L.*). Environ. Pollut. 266, 115391.
Ullah, H., Li, X., Peng, L., Cai, Y., Mielke, H.W., 2020. In vivo phytotoxicity, uptake, and translocation of PbS nanoparticles in maize (*Zea mays L.*) plants. Sci. Total Environ. 737, 139558.
Wang, C., Ma, L., Zhang, Y., Chen, N., Wang, W., 2021. Spatiotemporal dynamics of wetlands and their driving factors based on PLS-SEM: a case study in Wuhan. Sci. Total Environ., 151310
Wang, L., Han, X., Liang, T., Guo, Q., Li, J., Dai, L., Ding, S., 2019. Discrimination of rare earth element geochemistry and co-occurrence in sediment from Poyang Lake, the largest freshwater lake in China. Chemosphere 217, 851–857.
Wang, L., Liang, T., Zhang, Q., Li, K., 2014. Rare earth element components in atmospheric particulates in the Bayan Obo mine region. Environ. Res. 131, 64–70.
Wang, T.T., Ying, G.G., He, L.Y., Liu, Y.S., Zhao, J.L., 2020. Uptake mechanism, subcellular distribution, and uptake process of perfluorooctanoic acid and perfluorooctane sulfonic acid by wetland plant Alisma orientale. Sci. Total Environ. 733, 139383.
Xie, C., Guo, Z., Zhang, P., Yang, J., Zhang, J., Ma, Y., He, X., Lynch, I., Zhang, Z., 2022. Effect of CeO_2 nanoparticles on plant growth and soil microcosm in a soil-plant interactive system. Environ. Pollut. 300, 118938.
Yang, J., Cao, W., Rui, Y., 2017a. Interactions between nanoparticles and plants: phytotoxicity and defense mechanisms. J. Plant Interact. 12, 158–169.
Yang, L., Ren, H., Wang, M., Liu, N., Mi, Z., 2022. Assessment of eco-environment impact and driving factors of resident consumption: taking Jiangsu Province, China as an example. Resour. Environ. Sustain. 8, 100057.
Yang, X., Pan, H., Wang, P., Zhao, F.J., 2017b. Particle-specific toxicity and bioavailability of cerium oxide (CeO_2) nanoparticles to Arabidopsis thaliana. J. Hazard. Mater. 322, 292–300.
Younis, S.A., Kim, K.-H., Shaheen, S.M., Antoniadis, V., Tsang, Y.F., Rinklebe, J., Deep, A., Brown, R.J.C., 2021. Advancements of nanotechnologies in crop promotion and soil fertility: benefits, life cycle assessment, and legislation policies. Renew. Sustain. Energy Rev. 152, 111686.
Yu, X., Cao, X., Yue, L., Zhao, J., Chen, F., Wang, Z., Xing, B., 2020. Phosphate induced surface transformation alleviated the cytotoxicity of Y_2O_3 nanoparticles to tobacco BY-2 cells. Sci. Total Environ. 732, 139276.
Zhang, P., Guo, Z., Monikh, F.A., Lynch, I., Valsami-Jones, E., Zhang, Z., 2021. Growing rice (*Oryza sativa*) aerobically reduces phytotoxicity, uptake, and transformation of CeO_2 nanoparticles. Environ. Sci. Technol. 55, 8654–8664.
Zhang, P., Xie, C., Ma, Y., He, X., Zhang, Z., Ding, Y., Zheng, L., Zhang, J., 2017. Shape-dependent transformation and translocation of ceria nanoparticles in cucumber plants. Environ. Sci. Technol. Lett. 4, 380–385.
Zhao, L., Zhang, H., White, J.C., Chen, X., Li, H., Qu, X., Ji, R., 2019. Metabolomics reveals that engineered nanomaterial exposure in soil alters both soil rhizosphere metabolite profiles and maize metabolic pathways. Environ. Sci. Nano 6, 1716–1727.
Zhao, X., Zhang, W., He, Y., Wang, L., Li, W., Yang, L., Xing, G., 2021. Phytotoxicity of Y_2O_3 nanoparticles and Y^{3+} ions on rice seedlings under hydroponic culture. Chemosphere 263, 127943.